SUMMARY

The flow in an unequal elbow is typical of many flow configurations in which, as a sequel to separation, there is a reattachment of the detached stream to form a closed wake containing a standing eddy. A theoretical analysis of such a flow has been carried out by making an assumption regarding the distribution of vorticity, and by utilizing empirical data to establish the length of the wake. Both the detached stream and the separation region were embraced in the analysis, and attention was focused on the particular condition of large Reynolds Number R, for which the pattern and mechanism of flow are stable and insensitive to changes in R.

Good agreement has been obtained between the calculated and the experimentally observed flow patterns in the elbow configuration; and it is anticipated that the method of analysis will be equally successful if applied to other flow configurations in which separation occurs in a contracting stream.

NOTATION

M	Contraction ratio of the unequal elbow; and width of the broad limb.
U	Mean velocity in the upstream limb of the elbow.
ν	Kinematic viscosity.
R	Reynolds Number, $= MU/\nu$.
z	Physical plane containing the elbow configuration, $= x + iy$.
t	First transformed plane.
R'	Modulus on the t plane, $= \|t\|$.
c	Dimension OC on the t plane.
b	Dimension OB on the t plane.
s	Second transformed plane.
K	Vortex strength.
S_o	Position of the vortex in the upper half of the s plane, $= \|S_o\| . e^{i\theta}$.
$\overline{S_o}$	Position of the conjugate vortex in the lower half of the plane.
ω	Complex potential, $= \phi + i\psi$.
ω_1	Complex potential due to the point source in the s plane.
ω_2	Complex potential for the oblique immersion of a flat plate in an otherwise undisturbed vortex flow.
ϕ	Velocity potential.
ψ	Stream function.
PR	Pressure recovery on reattachment.
C_p	Pressure coefficient, $= \frac{\text{local pressure - ultimate downstream pressure}}{\text{total pressure drop across the elbow}}$.

1. Introduction

The traditional method of solving flow separation problems is to apply the classical free streamline theory proposed by Helmholtz (1868) in which the assumption is made that the pressure along the surface of separation is constant and equal to its downstream value. The extent to which the assumption is justified in a particular case determines the measure of agreement between the calculated flow pattern and the experimentally observed pattern. Generally, the assumption is not appropriate, particularly in cases where, as a sequel to separation, there is a reattachment of the detached stream to form a closed wake containing one or more standing eddies. If applied to such a flow configuration, the free streamline theory yields a particularly unsatisfactory description of the separation process as evidenced by the following characteristics:

(a) The profile of the dividing streamline is inaccurately defined,

(b) Reattachment is not simulated, and

(c) The flow within the separation region is not embraced in the analysis.

That the dividing streamline should be inaccurately defined is not surprising, because experimental observations reveal that the pressure along this contour is neither constant nor equal to the downstream pressure, as is assumed in the classical theory. In fact, the pressure in the wake near the separation point is considerably less than the downstream pressure, with the consequence that the observed width of the separation region is several percent less than the predicted width. Evidence of this was available even at the time the classical theory was introduced, Weisbach (1848) having observed and recorded the shapes of various separation surfaces. Some improvement regarding this aspect of the theoretical pattern is obtained if a modified

form of the classical analysis is used. Such a modification has been proposed by Roshko (1953) and is based on the assumption that the pressure in the initial part of the separation region is constant, but lower than the downstream pressure.

The classical and the Roshko models of flow do not describe the reattachment phenomenon and the circulatory flow within the separation region; neither do other existing potential flow solutions summarized by Lichtarowicz and Markland (1963) and by Robertson (1965). However, there is a need for a model which does simulate reattachment, and this has long been recognized. Batchelor (1956), for example, has stated that if a solution could be found which exhibits a closed separation region as Reynolds Number approaches infinity, then that would be regarded as preferable to the free streamline solution. An attempt to obtain such a solution is made in the present work, the flow configuration under consideration being that of a two-dimensional unequal elbow with separation at the inner corner.

Another limitation of existing potential flow models is that they do not satisfactorily describe the distribution of vorticity. Truesdale (1954) showed that the existence of only a small amount of viscosity may be of central importance in determining major flow characteristics; so that even in the limiting condition of vanishing viscosity, an accurate description of the residual vorticity is a prerequisite for a satisfactory solution. As evidenced by the widely differing models which have been proposed to describe the limiting flow, the main difficulty is in predicting this distribution of vorticity.

Batchelor assumed the existence of an inviscid stream with a uniform diffusion of vorticity confined to the separation region; and a similar distribution was predicted recently by Acrivos et al (1965). In contrast,

a different distribution in the separation region was suggested by the experimental data of Fromm (1963) and McGregor (1954). A concentration of vorticity was observed at the center of rotation of the circulatory flow, together with a tendency for the concentration to increase with the lessening of viscous action.

Concerning the vorticity associated with the surface of separation, the free streamline of the Helmholtz model is, in effect, a uniform and infinitely long vortex sheet, whereas the experiments of Fage and Johansen (1928) have demonstrated that the sheet rapidly decays and ultimately disappears. Further evidence supporting the concept of a decaying vortex sheet and also the concept of a concentration of the vorticity within the separation region was presented at a recent symposium reported by Küchemann (1965).

It may be concluded that available data strongly suggests that the most appropriate distribution of vorticity to be considered in the proposed theoretical model of flow is that of a concentration along the initial part of the dividing streamline and a separate concentration at the center of rotation of the standing eddy.

2. Transformation from the Physical Plane

The concentrations of vorticity are represented in the proposed model as a point vortex at the center of rotation of the eddy and as a vortex sheet along the dividing streamline (fig. 3). Apart from these singularities, the entire flow is irrotational, so that a potential flow analysis is appropriate throughout. It follows that the complex configuration and flow net of the physical plane can be conformally transformed by a Schwarz-Christoffel transformation into simpler geometry (the upper half of the t plane) where a study of the flow characteristics can be carried out more readily. The transformation grid, illustrated in figures 1 and 2, was derived from the following equations:

$$\frac{dz}{dt} = \frac{1}{\pi}(t+c)^{-1}\cdot(t+b)^{-\frac{1}{2}}\cdot(t)^{\frac{1}{2}} \qquad (1)$$

And consideration of the point I yields an expression for the contraction ratio

$$M = \left[c/(b-c)\right]^{\frac{1}{2}} \qquad (2)$$

The required transformation equation is obtained by integration and, with $t = 0$ at $z = 0$, is

$$\pi z = \log\left[t + \tfrac{b}{2} + \sqrt{t(t-b)}\right] + iM.\log\frac{\sqrt{c(t+b)}+\sqrt{(c-b)t}}{\sqrt{c(t+b)}-\sqrt{(c-b)t}} - \log\tfrac{b}{2} \qquad (3)$$

which can be simplified by putting $b = 2$ to fix the scale of the z plane. Hence

$$\pi z = \log\left[t + 1 + \sqrt{t(t-2)}\right] + iM.\log\frac{\sqrt{c(t+2)}+\sqrt{(c-2)t}}{\sqrt{c(t+2)}-\sqrt{(c-2)t}} \qquad (4)$$

where $M = \left[c/(2-c)\right]^{\frac{1}{2}}$ (5)

Note should be taken of the line in the z plane which is transformed into the 60° straight line of the t plane. It is this unique contour which marries with the elbow wall IO, from which it can be assumed that the flow initially separates along this path. Furthermore, experimental observations will be presented which reveal that the dividing streamline continues to follow this contour closely during the development of the separation region, so that the line is clearly the appropriate location of the vortex sheet in the z plane.

In the transformed flow of the t plane, the vortex sheet is linear, and this feature leads to a considerable simplification of the subsequent analysis of flow. Not many flow configurations exhibit this characteristic and, for the majority, the sheet lies along a curved path on the t plane. The unequal elbow is one of the few exceptions, and for a large range of contraction ratios ($2 \leqslant M \leqslant \infty$), the dividing streamline is observed to lie near

the 60^{o} line. This feature makes the elbow configuration particularly suitable for analysis, facilitating an assessment of the merits of the proposed potential flow model.

3. Potential Flow Model

Having derived the equation which gives the desired geometrical transformation from the z plane to the t plane, it is necessary to introduce into the upper half of the latter a suitable potential flow pattern. To do this, the vorticity elements associated with the separated flow are superimposed onto a uniform network of streamlines diverging from a point source (I) to a distributed sink at infinity (J), as shown in figure 3. The lower half of the t plane is assumed to contain a flow pattern symmetrical with that in the upper half.

At this point, the relative positions of the point source and the vortex sheet on the t plane must be clarified. Due to the logarithmic form of the t-z transformation equation (4), the length OA of the vortex sheet is much greater than the distance c of the point source from the origin and, indeed, the ratio will later be shown to be of the order of 10^{3}. Therefore, it is justified in all aspects of the analysis except the t-z transformation to treat the point source as if it were located at the origin of the t plane.

Some assumption has to be made regarding the distribution of vorticity along the vortex sheet in the t plane, and in fact the behavior of the sheet is assumed to be the same as if there were an impermeable plate immersed in the fluid. This assumption is appropriate since it yields a realistic simulation of the relative motion on the two sides of the sheet, together with the attainment of a common velocity at the downstream extremity. Therefore, in the analysis which follows, the line OA in the t plane is considered to be the location of a flat plate giving a smooth separation of flow at A. For convenience, the scale of the t plane is adjusted so that the line has unit

length with its end at $t = e^{i\pi/3}$.

This treatment of the vortex sheet enables a further simplifying transformation to be carried out, viz., the $t-s$ transformation. It enables the V-shaped plate in the t plane, formed by the flat plate along OA and by a similar plate along the mirror image of OA below the axis, to be transformed into another plate O'AO lying on the axis of the s plane. The Schwarz-Christoffel equation is

$$\frac{dt}{ds} = (s+1)\cdot(2s)^{2/3}\cdot(s+3)^{1/3} \tag{6}$$

which is integrated to give the desired transformation equation

$$t = s^{1/3}\cdot\left(\frac{s+3}{2}\right)^{2/3}. \tag{7}$$

The upper half of the t-s transformation grid is depicted in figure 4.

Figure 5 shows the geometrical configuration of the s plane together with the potential flow elements transformed from the t plane. The elements comprise a vortex doublet, K and $-K$, an impermeable plate O'AO, a point source of strength $2MU$ at the end of the plate, and a distributed sink at infinity. Referring to the symbols defined in figure 5, it is clear that the resultant flow pattern is determined by the position of the doublet, $|s_o|\cdot e^{i\theta}$ and $|s_o|e^{-i\theta}$, and by its strength relative to that of the point source K/MU. In effect, the three quantities $|s_o|$, θ and K/MU require evaluation, and this is done in the course of satisfying the following requirements.

1. In the t plane, the fluid velocity at the tip of the plate is finite but not zero, and in the s plane too, the corresponding point (A at $s = -1$) marks the inception of the dividing streamline. The equation describing this feature of the final flow pattern is derived in §4, and serves as one of the three required to evaluate the quantities enumerated in the previous paragraph.

2. The composite flow pattern in the s plane is clearly a symmetrical one with the plate O'AO lying on the axis of symmetry and hence along one of the streamlines. Despite this, the plate has a considerable bearing on the equilibrium of the potential flow elements, each one of which must be stationary under the action

of the others; e.g., the velocity of each concentrated vortex must be zero in two mutually perpendicular directions. The two equations describing this equilibrium condition are derived in §5, and serve to complete the evaluation of $|s_0|$, θ, and K/MU.

4. Condition for Smooth Separation

It has been established that smooth separation from the tip of the plate in the t plane is ensured if, in the s plane, inception of the dividing streamline occurs at the point A ($s = -1$). The following derivation is of an equation to describe this condition.

The complex potential ω describing the arrangement of flow elements shown in figure 5 is

$$\omega = -\frac{MU}{\pi}.\log(s+3) - \frac{iK}{2\pi}.\log\frac{s-s_0}{s-\bar{s}_0} \tag{8}$$

from which

$$\frac{d\omega}{ds} = -\frac{MU}{\pi}.\frac{1}{s+3} - \frac{iK}{2\pi}.\left[\frac{s_0-\bar{s}_0}{(s-s_0)(s-\bar{s}_0)}\right] \tag{9}$$

The magnitude of the velocity at any point in the t plane = $\left|\frac{d\omega}{dt}\right|$, and at the tip of the plate where $t = e^{i\pi/3}$, corresponding to $s = -1$, the velocity magnitude = $\left|\frac{d\omega}{dt}\right|_A$ where

$$\left|\frac{d\omega}{dt}\right|_A = \left|\frac{d\omega}{ds}\right|_A \Big/ \left|\frac{dt}{ds}\right|_A \tag{10}$$

The intention is to satisfy the condition for this to be finite and non-zero. It is clear from equation (6) that the denominator is zero at $s = -1$, and, therefore, for the above ratio to be finite, the numerator must also be zero. In other words, for the plate tip velocity to be finite

$$\left|\frac{d\omega}{ds}\right|_A = 0$$

Therefore, from equation (9),

$$\frac{K}{MU} = \frac{i(1+s_0)(1+\bar{s}_0)}{s_0-\bar{s}_0} \tag{11}$$

Equation (11) describes the condition for a finite separation velocity from

the tip of the plate, and the following derivation is of an equation for the magnitude of this velocity, $\left|\frac{d\omega}{dt}\right|_A$

Initially, it is indeterminate, since both $\left|\frac{d\omega}{ds}\right|_A$ and $\left|\frac{dt}{ds}\right|_A$ are zero, and it must, therefore, be evaluated from the ratio of the second differential coefficients.

$$\left|\frac{d\omega}{dt}\right|_A = \left|\frac{d^2\omega}{ds^2}\right|_A \Big/ \left|\frac{d^2t}{ds^2}\right|_A$$

From equation (9)

$$\frac{d^2\omega}{ds^2} = \frac{MU}{\pi} \cdot \frac{s_0\bar{s}_0 + 3(s_0 - s) + 3(\bar{s}_0 - s) - s^2}{(s+3)^2 \cdot (s_0 - s)(\bar{s}_0 - s)} .$$

$$\left|\frac{d^2\omega}{ds^2}\right|_A = \frac{MU}{\pi} \cdot \frac{s_0\bar{s}_0 + 3s_0 + 3\bar{s}_0 + 5}{4(s_0+1)(\bar{s}_0+1)} .$$

And from equation (6)

$$\frac{d^2t}{ds^2} = -(2)^{1/3} \cdot (s)^{-5/3} \cdot (s+3)^{-4/3}$$

$$\left|\frac{d^2t}{ds^2}\right|_A = \frac{1}{2} .$$

Hence, the magnitude of the plate tip velocity $\left|\frac{d\omega}{dt}\right|_A = \frac{MU}{2\pi} \cdot \frac{s_0\bar{s}_0 + 3s_0 + 3\bar{s}_0 + 5}{(s_0+1)(\bar{s}_0+1)}$ (12)

5. Conditions for Equilibrium

For equilibrium of the various elements constituting the potential flow in the s plane, each one must be stationary under the action of the others, and in particular, there must be equilibrium of the doublet, or rather of either one of the two symmetrical vortices which constitute the doublet. In fact, the equilibrium of the vortex in the upper half of the plane is investigated by considering the interaction at the vortex center of the source and the conjugate vortex.

The flow pattern due to the point source is unaffected by the presence of the flat plate since the latter lies along one of the streamlines diverging radially away. The pattern is unique and independent of the strength of the source, a typical streamline being that shown as a broken line passing through O' in figure 6 .

The separate pattern due to the conjugate vortex is also unique and independent of the strength, but as the figure shows, the presence of the flat plate now has an important bearing on the flow pattern. It causes a severe distortion of the streamlines, which would otherwise form concentric circles, and it causes the direction of flow at the conjugate point to deviate from the horizontal. Indeed, for the particular vortex position depicted in the figure, the flow at the conjugate point is directed towards O' and is exactly opposite that due to the point source. This feature does not apply in general, but only for certain vortex positions, the locus of which is obtained by computation from the equations given in the appendix, and is shown in the figure as a broken line passing through the chosen vortex position.

Clearly, for the conjugate point to be stationary under the interaction of the source and the active vortex, the latter must lie along the equi-direction locus regardless of the magnitudes of these two elements of the flow. The second condition requires that the velocity due to the source be the same in magnitude as that due to the vortex, and it differs from the first condition in that the magnitude of the K/MU parameter is now important. In order to make the conjugate point stationary, each point on the locus must be associated with a particular value of the parameter, and the combination which is chosen is that which simultaneously satisfies equation (11) resulting in a smooth separation from the tip of the wall in the t plane.

The required position for the vortex in the upper half of the s plane is at $|s_v| = 0.444$ and $\Theta = 88^\circ 33'$, and the value of K/MU associated with it is 1.373. The corresponding flow in the t plane is illustrated in fig. 7.

6. Final Flow Pattern

The locating of the vortex doublet and the evaluating of the K/MU ratio enable the final potential flow pattern to be derived in the s and t planes

using equations (8) and (7), respectively. The flow relating to the upper half of the symmetrical t plane is shown in figure 8, and it is this pattern which is subsequently transformed to the elbow configuration of the z plane. However, before the transformation can be carried out, the scale of the t plane must be established. This is done in the course of making the length of the potential flow separation region the same as the length of the separation region observed experimentally.

The experiments formed part of an earlier investigation (1962) of flow separation and reattachment in an unequal elbow, and included a flow visualization study and the measurement of pressure and shear stress along the wall bounding the separation region. Visual observations enabled the initial part of the dividing streamline to be located, but the downstream part was obscured by turbulence so that recourse to pressure and shear stress measurements had to be made in order to throw light on the nature of the reattachment. In fact, the latter is always characterized by a sharp pressure recovery, an example of which is illustrated in figure 9 for an elbow having a 5/1 contraction ratio and for Reynolds Number in the range 9,440 to 18,170. Throughout this wide range, the effect of R on the wall pressure distribution was very small, from which it appears likely that further increase in R would not greatly affect the distribution.

The exact point of reattachment along a wall is characterized by the absence of shear stress, and in the experiments for the elbow, the desired point was located in this way. For the same range of R as that which related to the pressure results, shear stress measurements indicated that reattachment occurred at a point corresponding to $z = 2.2$. Its position is probably the same for all large Reynolds Numbers, so that the constancy of the length of the separation region makes this empirical dimension an

appropriate one to introduce into the potential flow solution. Incidentally, the pressure recovery at the observed reattachment point was 0.75 complete, as shown in the figure, and this is consistent with the results of Nash (1963) who, for a variety of configurations, found the same degree of completeness of the reattachment pressure recovery at the point of zero shear stress along the wall.

Also associated with reattachment is a high level of turbulent mixing, and since the present state of knowledge does not enable the point of inception to be predicted theoretically, recourse would have to be made to experiment if its location were required. It is not surprising, therefore, that the location of the reattachment point must also be established experimentally, as is the case here. In fact, a scale of 1750 has to be introduced to the t plane, so that when the flow is transformed to the z plane, the reattachment point is in the desired position. Point A will, therefore, be located at $t = 1750.e^{i\pi/3}$, the concentrated vortex at $t = 1767.e^{0.613\,i}$, the reattachment point at $t = 3623$, and the point source at $t = -1.923$.

The final transformation yields the flow pattern illustrated in the upper part of figure 9. It reveals the closeness of the profile of the vortex sheet to that of the observed dividing streamline, and also demonstrates the circulatory flow in the separation region and the downstream reattachment. Unfortunately, there is no experimental evidence available for the elbow which gives the position of the center of rotation of the circulatory flow in the separation region. And it appears that the most suitable comparitor against which the calculated vortex position ($z = 1.982.e^{0.098\,i}$) can be compared is the data of McGregor who, for the separation region on an airfoil, located a powerful vortex at the downstream end of the region, and in a similar relative position to that calculated for the vortex center in the elbow. Nor

are there any experimental results available for the velocity variation along the dividing streamline with which to compare the calculated velocity at the end of the vortex sheet. (The latter, computed from equation (12) and expressed as a fraction of the ultimate velocity in the downstream limb of the elbow, is 2.16).

In conclusion, it may be stated that the final flow pattern illustrated in figure 10 confirms that the proposed potential flow model gives a realistic representation of the flow separation and reattachment in an unequal elbow. It is anticipated that the model will also be appropriate for the solution of other problems in which the flow separation occurs in a contracting stream. (An example of such a configuration is the entrance to a pipe from a reservoir). Flow separation in an expansive flow is likely to be less suitable because of difficulties in locating the reattachment point and in defining the vortex sheet.

The project was carried out at the University of Pittsburgh, as part of a NASA Post-Doctoral Fellowship, and data was processed at the University Computation Center under a grant from the National Science Foundation, (G 11309).

REFERENCES

Acrivos, A., Snowden, D. D., Grove, A. S., and Petersen, E. E. 1965 The steady separated flow past a circular cylinder at large Reynolds Numbers. J. Fluid Mech. 21, 737.

Batchelor, G. K. 1956 A proposal concerning laminar wakes behind bluff bodies at large Reynolds Numbers. J. Fluid Mech. 1, 388.

Duggins, R. K. 1962 A study of flow in a plate valve. Ph.D. Thesis, University of Nottingham.

Fage, A. and Johansen, F. C. 1928 The structure of vortex sheets. Phil. Mag. S7, 5, 417.

Fromm, J. E. 1963 A method for computing non-steady, incompressible, viscous fluid flows. Los Alamos Scientific Laboratory Report LA 2910.

Helmholtz, H. 1868 On discontinuous fluid motions. Phil. Mag. 4, 36, 337.

Küchemann, D. 1965 Report on the I.U.T.A.M. Symposium on concentrated vortex motions in fluids. J. Fluid Mech. 21, 1.

Lichtarowicz, A. and Markland, E. 1963 Calculation of potential flow with separation in a right-angled elbow with unequal branches. J. Fluid Mech. 17, 596.

McGregor, I. 1954 Regions of localized boundary layer separation and their role in the nose-stalling of aerofoils. Ph.D. Thesis. University of London, QMC.

Nash, J. F. 1963 An analysis of two-dimensional turbulent base flow, including the effect of the approaching boundary layer. A.R.C., R. and M. 3344.

Robertson, J. M. 1965 Hydrodynamics in theory and application. Prentice Hall.

Roshko, A. 1953 A new hodograph for free-streamline theory. NACA TN 3169.

Truesdale, C. A. 1954 Kinematics of vorticity. University of Indiana. Science Series, 19.

Weisbach, J. 1848 Principles of the mechanics of machinery and engineering. Vol. 1. Lee and Blanchard. Philadelphia.

APPENDIX

Further to the discussion in § 5 , the calculation is given for the location of the desired stationary point conjugate to one active vortex in the lower half of the **s** plane.

The complex potential ω_1 due to the point source is unaffected by the presence of the flat plate, and is

$$\omega_1 = \frac{MU}{\pi} \log(s+3) \tag{A1}$$

But the presence of the plate is significant in the case of the active vortex for which the flow pattern is derived from the potential flow solution to the problem of a flat plate normal to a uniform stream. The complex potential ω_2 at a point α in such a stream moving with undisturbed velocity U past a flat plate of length $2\alpha_1$ is given by equation (A2) which, together with the required transformation equations, is included in Table 1.

$\omega_2 = \frac{2iU}{\alpha_1}\sqrt{\alpha-\alpha_1}\sqrt{\alpha+\alpha_1}$ where $U = \frac{K\alpha_1}{4\pi}$.	$\frac{d\omega_2}{d\alpha} = \frac{iU}{\alpha_1}\left[\sqrt{\frac{\alpha-\alpha_1}{\alpha+\alpha_1}} + \sqrt{\frac{\alpha+\alpha_1}{\alpha-\alpha_1}}\right]$ (A2)
$\alpha = \log \beta$	$\frac{d\alpha}{d\beta} = \frac{1}{\beta}$
$\gamma = -2\beta \operatorname{csch}\alpha_1 + 2\coth\alpha_1$	$\frac{d\gamma}{d\beta} = -2\operatorname{csch}\alpha_1$
$\gamma = \delta + \frac{1}{\delta}$	$\frac{d\gamma}{d\delta} = 1 - \frac{1}{\delta^2}$
$\varepsilon = \delta . e^{i\phi}$	$\frac{d\varepsilon}{d\delta} = e^{i\phi}$
$\zeta = \varepsilon + \frac{1}{\varepsilon}$	$\frac{d\zeta}{d\varepsilon} = 1 - \frac{1}{\varepsilon^2}$
$s = 0.75(\zeta - 2)$	$\frac{ds}{d\zeta} = 0.75$

Table 1. The equations transform the simple configuration of the α plane into

the s plane to give the flow pattern resulting from the oblique immersion of a flat plate in an otherwise undisturbed vortex flow. α_1 and ϕ define the position of the plate relative to the vortex.

The velocity at any point in the s plane due to the single active vortex is given by $\frac{d\omega_2}{ds}$ computed from the differential coefficients in the table. Corresponding to this for the point source is the expression $\frac{d\omega_1}{ds}$ defined by equation (A1), and in the equilibrium condition, $\frac{d\omega_1}{ds} = -\frac{d\omega_2}{ds}$ at the point conjugate to the vortex.

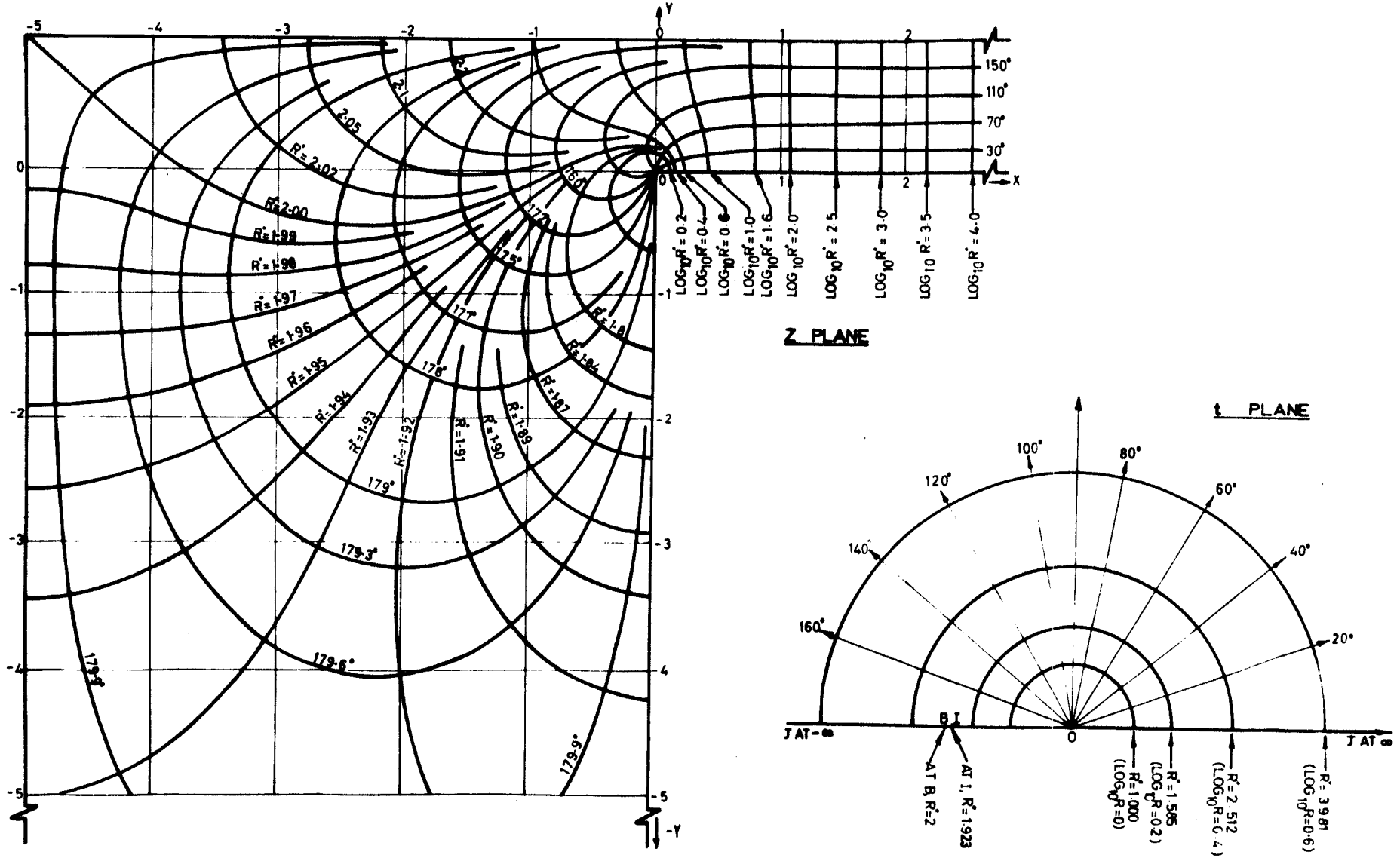

Figure 1. **t-z TRANSFORMATION**

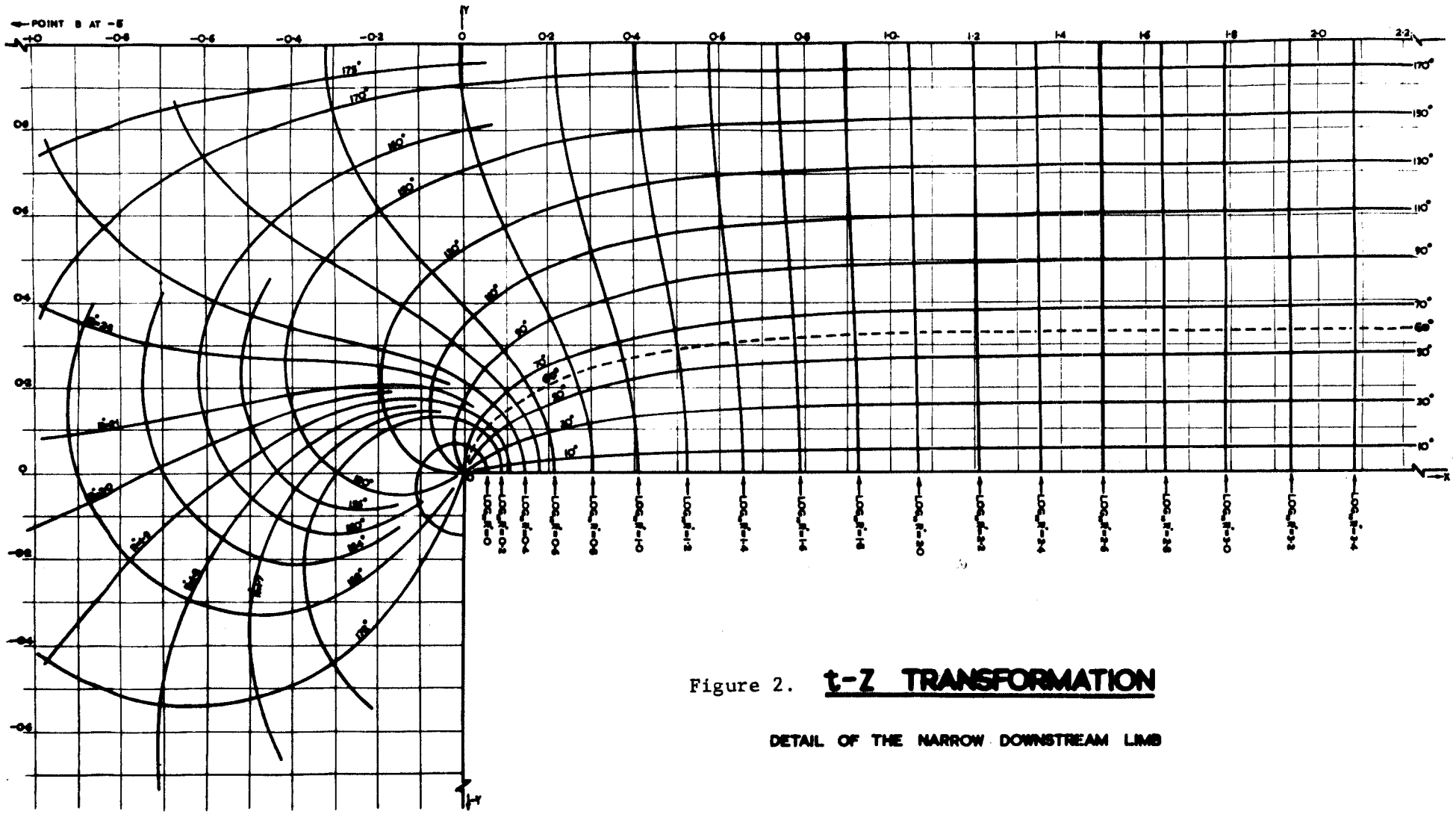

Figure 2. **t-Z TRANSFORMATION**

DETAIL OF THE NARROW DOWNSTREAM LIMB

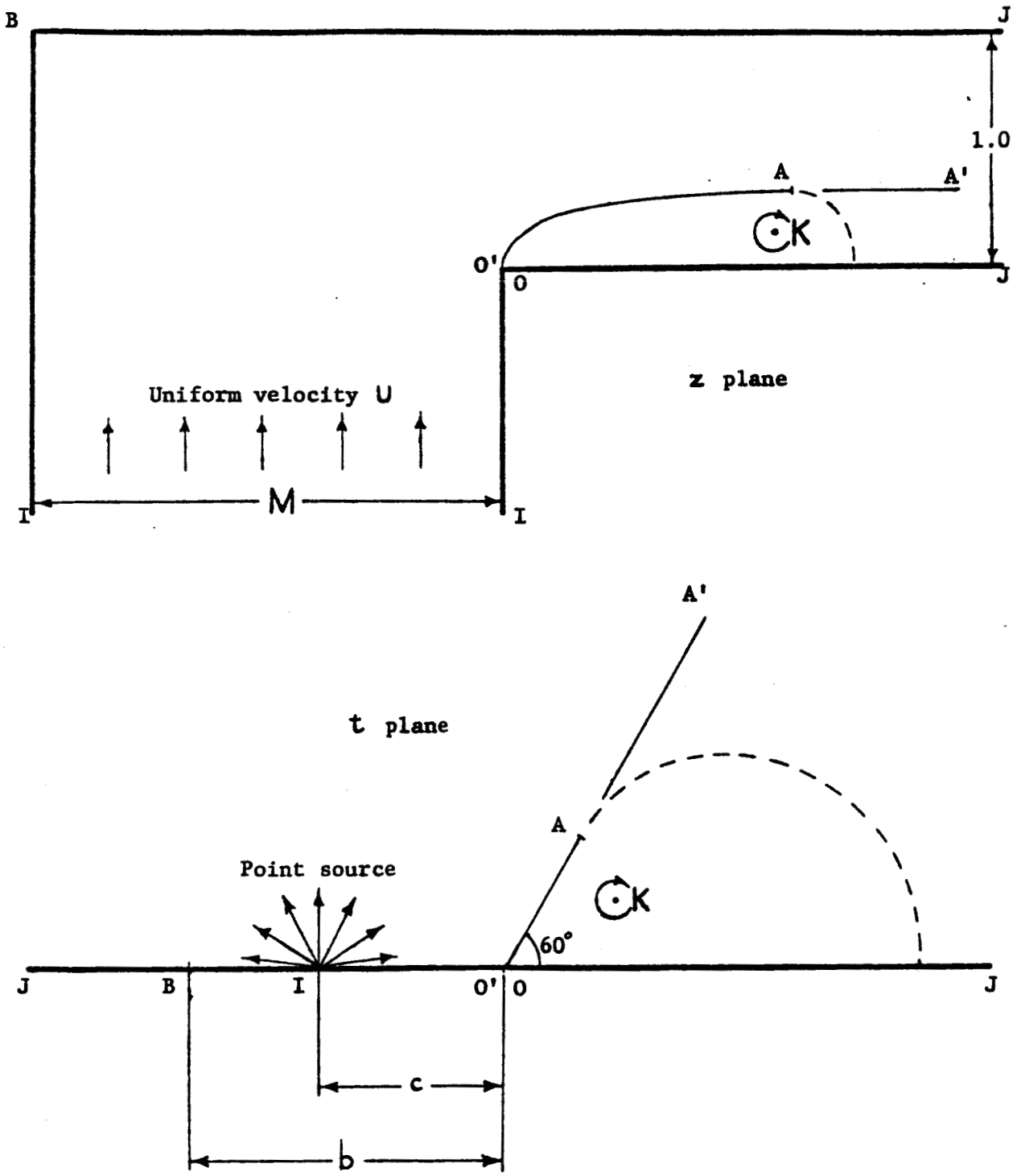

Figure 3. The z-t transformation. A vortex sheet lies between O and A along the 60° contour OAA'.

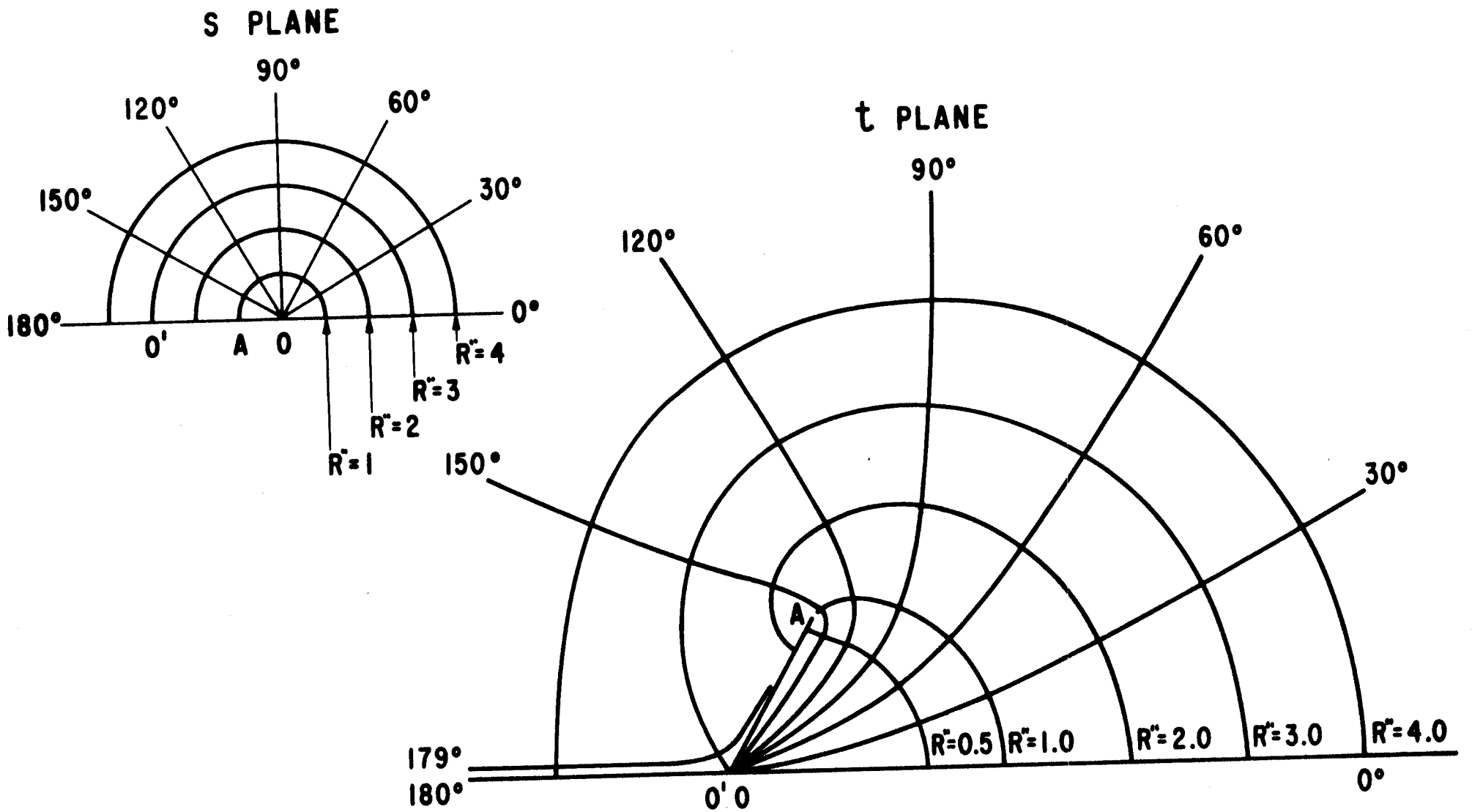

Figure 4. **s-t TRANSFORMATION.**

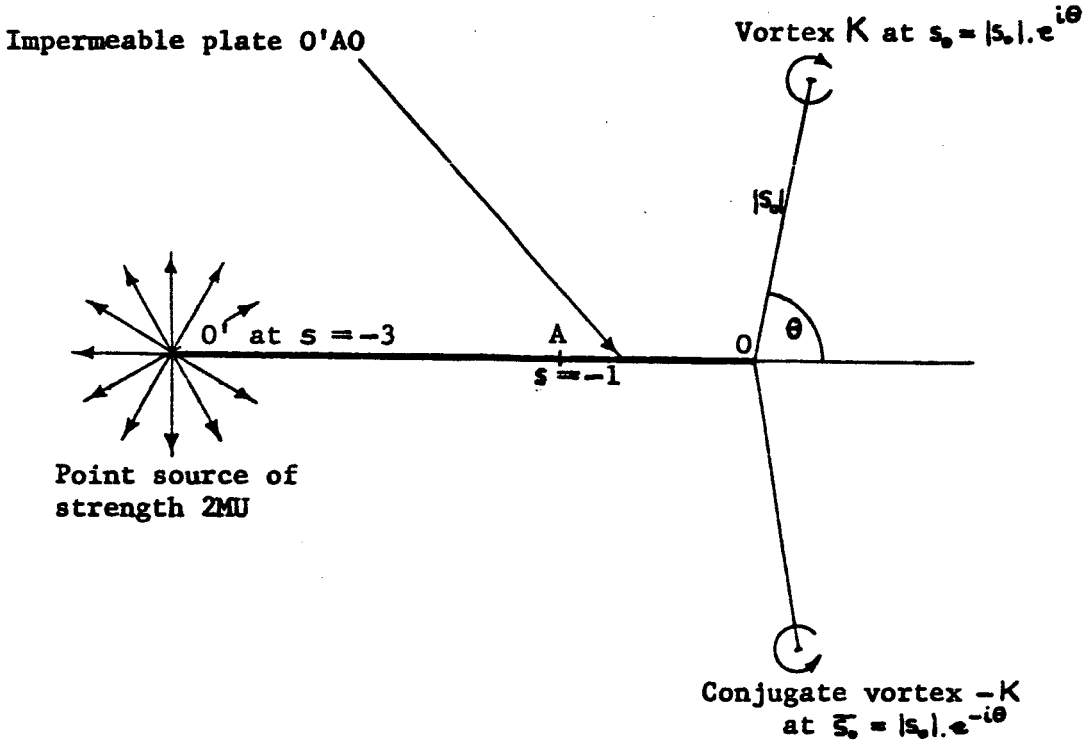

Figure 5. The s plane, illustrating the arrangement of the elements of the potential flow.

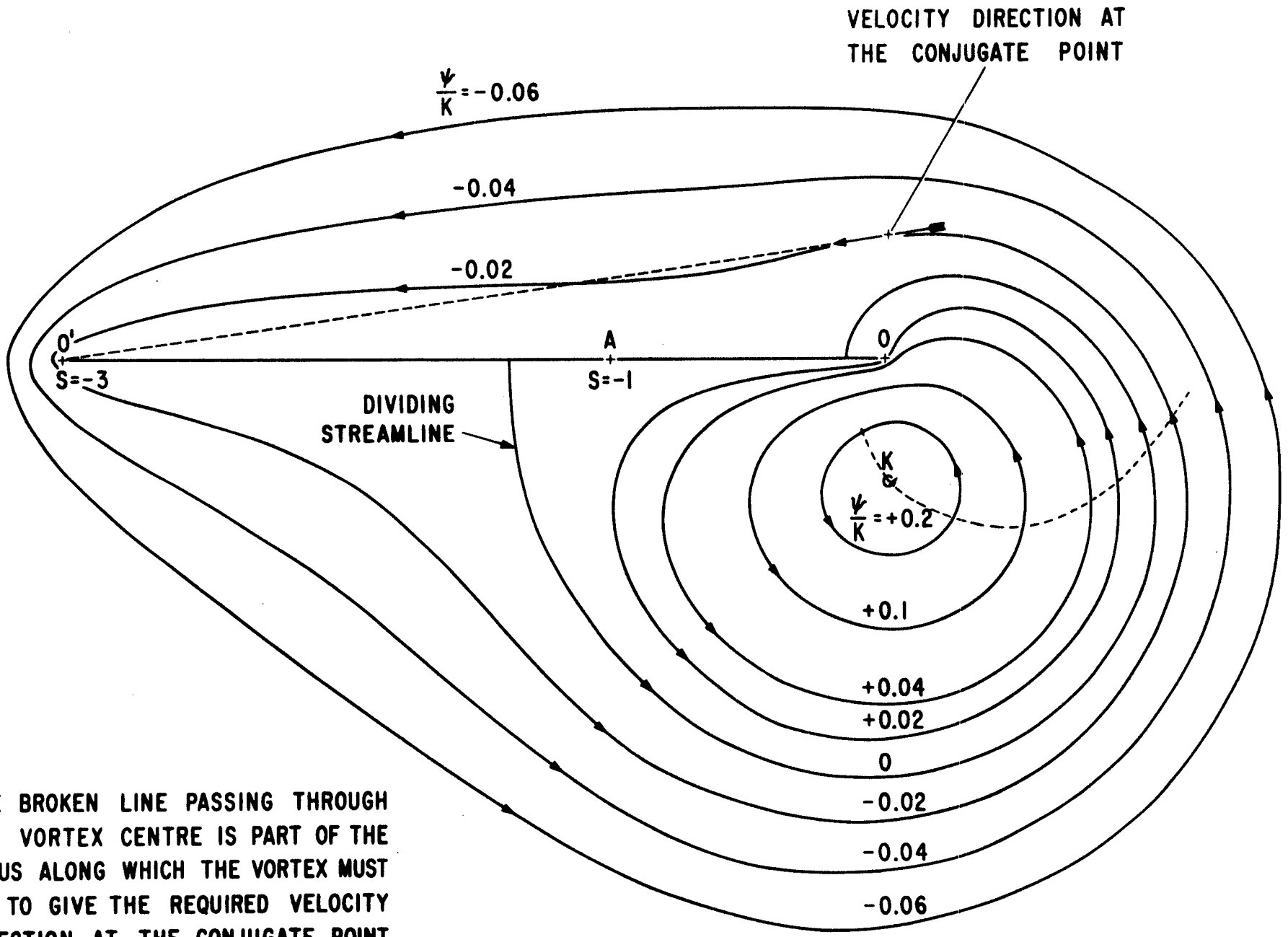

THE BROKEN LINE PASSING THROUGH THE VORTEX CENTRE IS PART OF THE LOCUS ALONG WHICH THE VORTEX MUST LIE TO GIVE THE REQUIRED VELOCITY DIRECTION AT THE CONJUGATE POINT.

Figure 6

STREAMLINES FOR A SINGLE VORTEX ON THE S PLANE.

ψ is the stream function

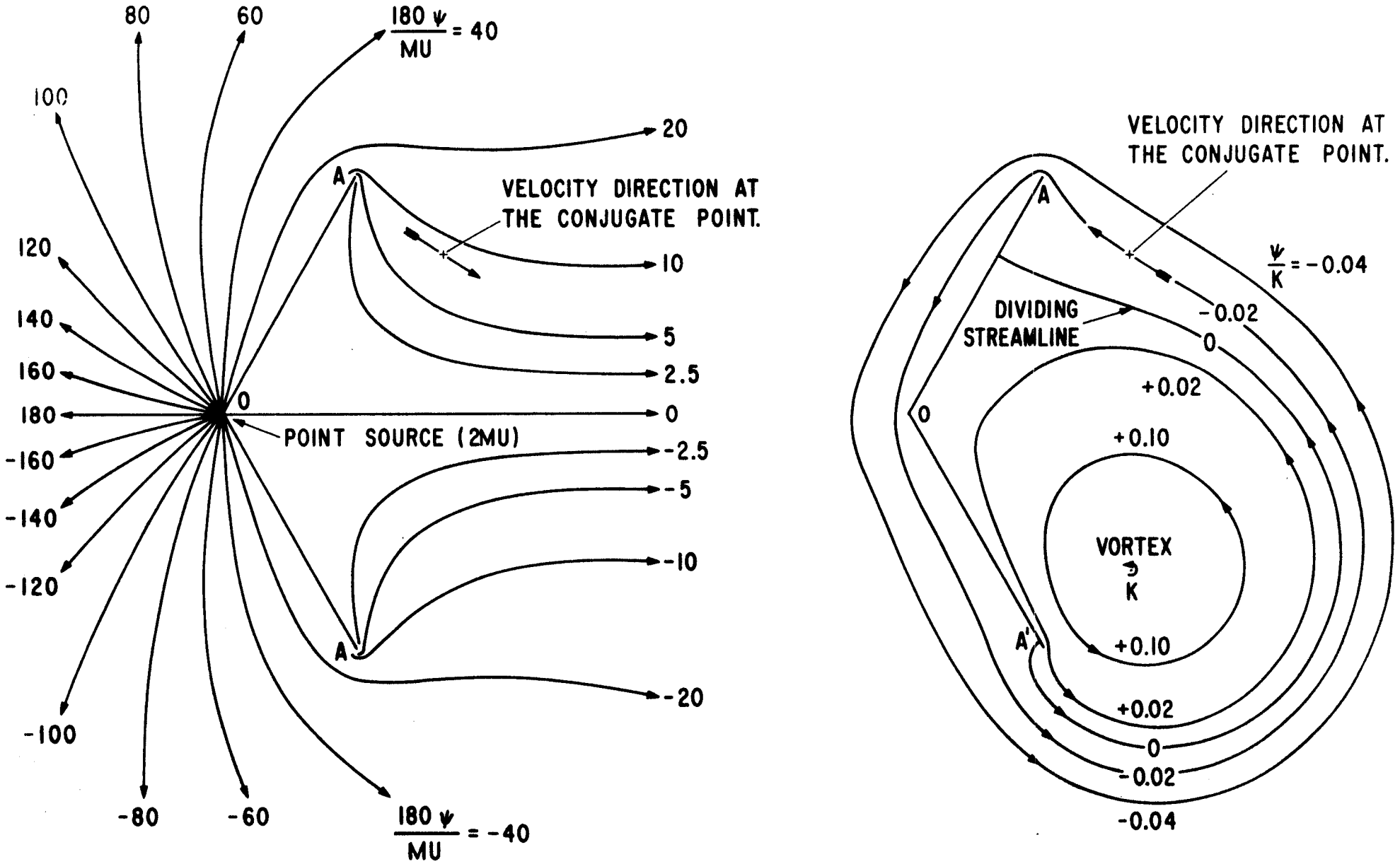

Figure 7

THE SOURCE AND CONJUGATE VORTEX COMPONENTS OF THE FLOW PATTERN.

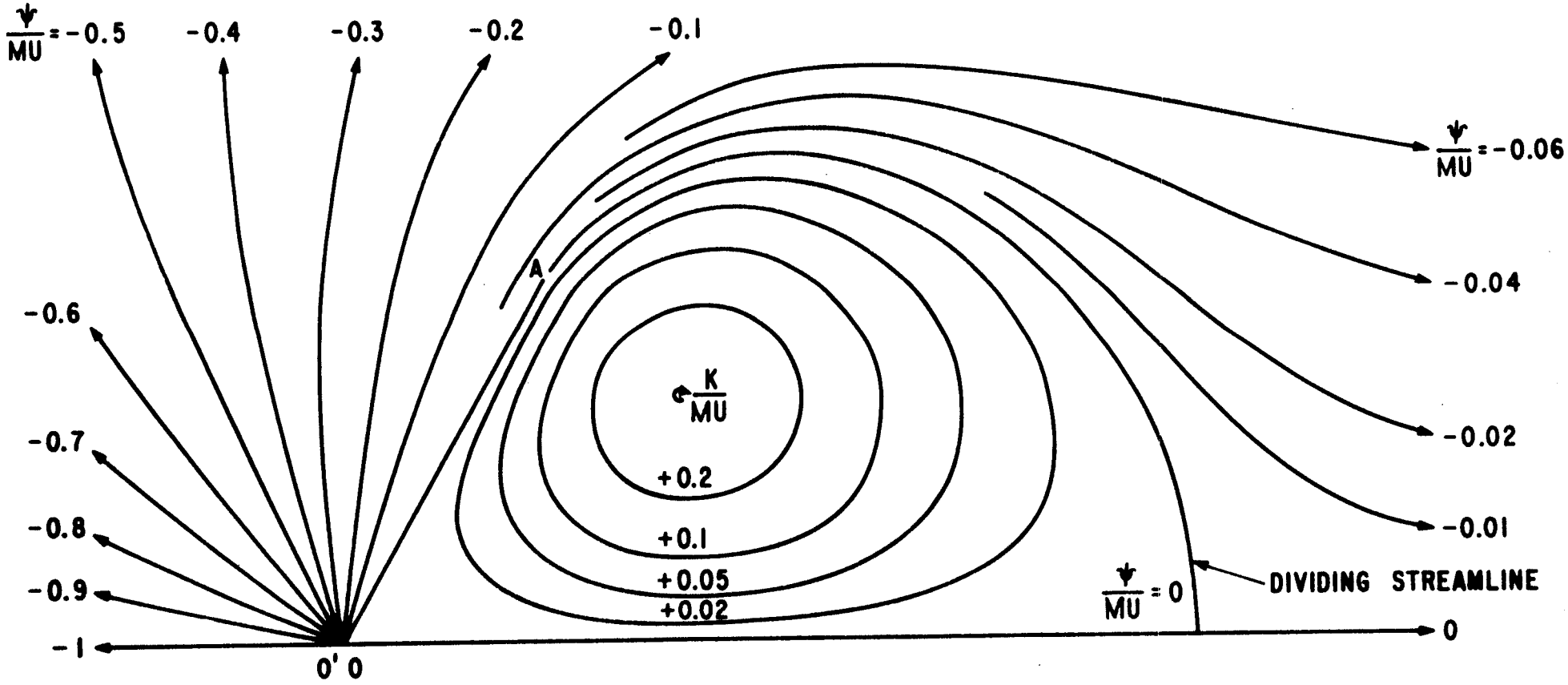

Figure 8. STREAMLINES IN THE UPPER HALF OF THE t PLANE.

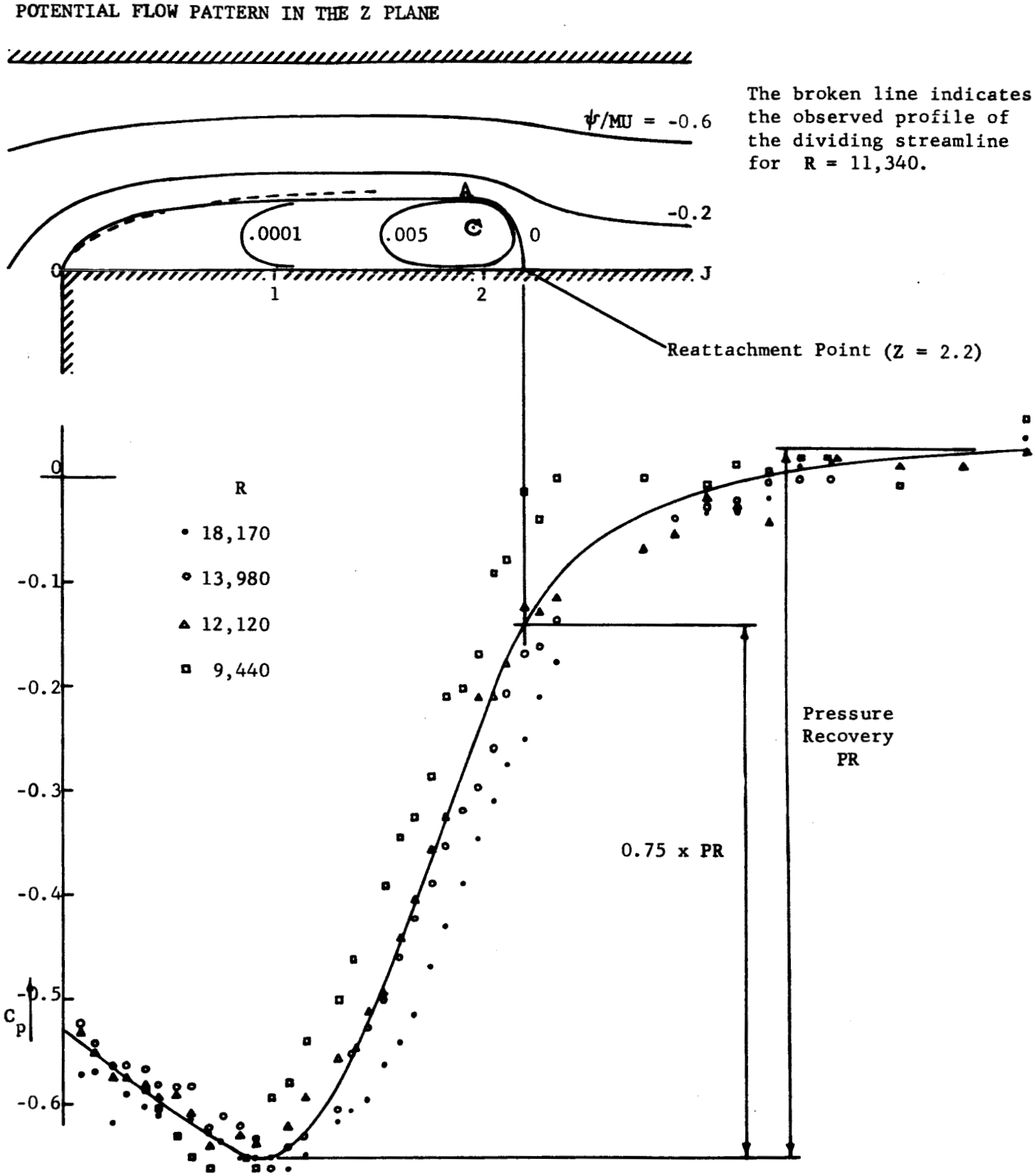

Figure 9

EXPERIMENTALLY MEASURED PRESSURE DISTRIBUTION FOR THE WALL OJ OF THE UNEQUAL ELBOW

Pressure Coefficient, $C_p = \frac{\text{Local Pressure - Ultimate Downstream Pressure}}{\text{Total Pressure Drop Across the Unequal Elbow}}$

Reynolds Number, $R = MU/\nu$ where ν is the kinematic viscosity

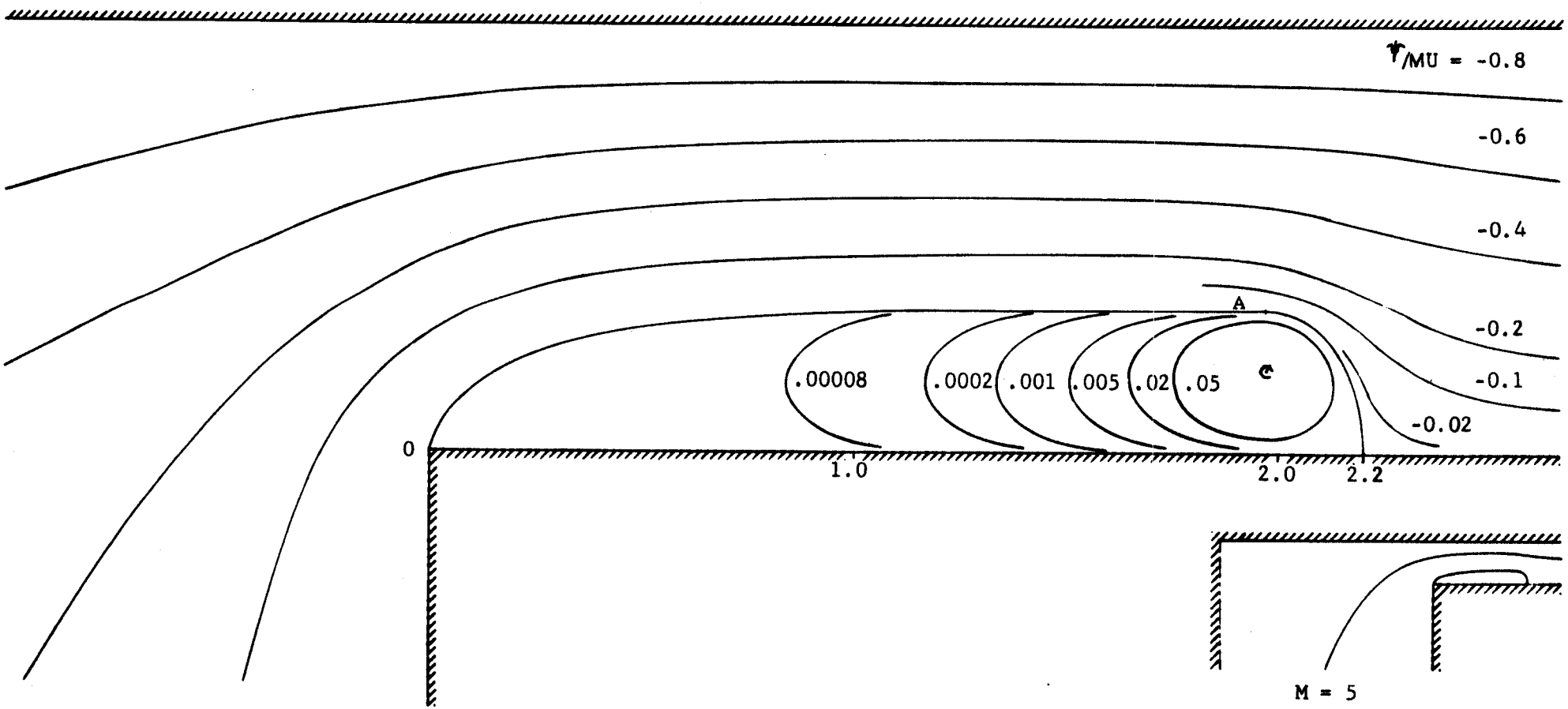

Figure 10. POTENTIAL FLOW PATTERN IN THE Z PLANE